Published in final edited form as:
Nat Struct Mol Biol. ; 18(12): 1400–1407. doi:10.1038/nsmb.2172.

The E3 ubiquitin ligase RNF8 stabilizes TPP1 to promote telomere end protection

Rekha Rai[1,+], **Ju-Mei Li**[2,+], **Hong Zheng**[3], **Gabriel Tsz-Mei Lok**[4], **Yu Deng**[5], **Michael Huen**[4,7], **Junjie Chen**[6,7], **Jianping Jin**[2], and **Sandy Chang**[1,*]

[1]Department of Laboratory Medicine, Yale University School of Medicine 330 Cedar St. New Haven, CT 06520

[7]Department of Therapeutic Radiology Yale University School of Medicine 330 Cedar St. New Haven, CT 06520

[2]Department of Biochemistry and Molecular Biology University of Texas Health Science Center Houston TX 77030

[3]Department of Lymphoma Research, The M.D. Anderson Cancer Center 1515 Holcombe Blvd. Houston, TX 77030 USA

[5]Department of Genetics, The M.D. Anderson Cancer Center 1515 Holcombe Blvd. Houston, TX 77030 USA

[6]Department of Experimental Radiation Oncology The M.D. Anderson Cancer Center 1515 Holcombe Blvd. Houston, TX 77030 USA

[4]Genome Stability Research Laboratory University of Hong Kong L1, Laboratory Block 21 Sassoon Road, Pokfulam, Hong Kong

Abstract

TPP1, a component of the mammalian shelterin complex, plays essential roles in telomere maintenance. It forms a heterodimer with POT1 to repress ATR-dependent DNA damage signaling at telomeres, and recruits telomerase to chromosome ends. Here we show that the E3 ubiquitin ligase RNF8 localizes to and promotes the accumulation of DNA damage proteins 53BP1 and γ-H2AX to uncapped telomeres. TPP1 is unstable in the absence of RNF8, resulting in telomere shortening and chromosome fusions via the alternative non-homologous end joining (A-NHEJ)-mediated DNA repair pathway. The RNF8 ubiquitin ligase RING domain is essential for TPP1 stability and retention at telomeres. RNF8 physically interacts with TPP1 to generate Ubc13-dependent K63 polyubiquitin chains that stabilizes TPP1 at telomeres. The conserved TPP1 lysine residue 233 is essential for RNF8-mediated TPP1 ubiquitylation and localization to telomeres. Our results demonstrate that TPP1 is a novel substrate for RNF8, and suggest a previously unrecognized role for RNF8 in telomere end protection. We propose a model in which engagement of classical vs. A-NHEJ repair pathways at dysfunctional telomeres is controlled by the ubiquitin ligase functions of RNF8.

[*]To whom correspondence should be addressed: schang@yale.edu.
[+]These authors contributed equally to this work

Author Contributions RR, JJ, and SC conceived the project and designed the experiments. RR, JJ, JML, HZ performed the experiments and generated data for the figures. YD generated anti-mouse TPP1 antibody. JC provided *Rnf8*$^{-/-}$ mice and anti-human RNF8 antibody. MH and GTML provided human RNF8 cDNAs and shared unpublished results. RR, JJ, and SC analyzed and interpreted the data. RR and SC composed the figures and wrote the paper.

Introduction

In mammals, telomeres consist of TTAGGG repetitive sequences that provide both end-protection and a mechanism for the maintenance of chromosomal ends. Telomeres are bound and stabilized by duplex telomere binding proteins TRF1 and TRF2-RAP1, the single-stranded telomere binding protein POT1 and the adapter protein TIN2[1]. POT1 in turn interacts with TPP1 to form the TPP1-POT1 heterodimer, a protein complex that plays critically important roles in telomere maintenance and end protection[2–4]. Dysfunctional telomeres that can no longer exert end-protective functions are recognized as DNA double stranded breaks (DSBs) by the DNA damage repair (DDR) pathway. Disruption of the TPP1-POT1 protein complex activates an ATR-dependent DNA damage checkpoint response at telomeres, resulting in the engagement of alternative non-homologous end joining (A-NHEJ) repair pathway to mediate chromosome end-to-end fusions[4–7]. A-NHEJ-mediated repair of DSBs have been implicated in cancer formation by promoting oncogenic chromosomal translocations and deletions[8,9].

The sensing of DSBs involves a series of post-translational protein modifications, including phosphorylation, methylation, acetylation and ubiquitylation[10,11]. Recent studies reveal that protein ubiquitylation plays important regulatory roles at DSBs to influence both the efficiency and specificity of DNA repair. Importantly, localization of DDR proteins including 53BP1, BRCA1, Brcc36, Abraxas and Rap80 to DSBs requires the E3 ubiquitin ligases RNF8 and RNF168[12–15]. RNF8 contains two conserved domains-a FHA domain that binds phosphopeptides and a RING domain essential for its ubiquitin ligase activity. RNF8 is recruited to damage sites through interaction of its FHA domain with ATM-phosphorylated MDC1. In conjunction with its E2 ubiquitin conjugating enzyme UBC13, the RNF8 RING domain catalyzes the formation of polyubiquitin chains composed of lysine-63 (K63) polyubiquitin linkages on histones H2A and H2AX. This in turn sets up a permissive environment for the recruitment of RNF168, a second E3 ubiquitin ligase, to amplify the RNF8-initiated damage signal. Therefore, RNF8 serves as an adaptor that physically integrates phosphorylation and ubiquitylation-dependent DSB signaling[11]. RNF8 is also able to generate lysine-48 (K48) polyubiquitin linkages on itself, a modification usually associated with proteosome mediated degradation[16].

While RNF8 plays an active role in the signaling of DSBs, other substrates of RNF8 besides histones are currently unknown. In this report, we show that TPP1 is unstable in the absence of the E3 ubiquitin ligase RNF8, resulting in rapid telomere shortening and chromosome fusions. The RNF8 ubiquitin ligase function is essential for TPP1 stability and its localization to telomeres. We also show that RNF8 physically interacts with TPP1 to generate Ubc13 dependent K63 polyubiquitin chains that stabilizes TPP1 at telomeres. Our results demonstrate that TPP1 is a substrate for RNF8, and suggest a previously unrecognized role for RNF8 in the regulation of classical vs. alternative non-homologous end joining repair pathways at dysfunctional telomeres.

Results

RNF8 mediates the DNA damage response at dysfunctional telomeres

The importance of RNF8 for the recruitment of DNA damage factors to sites of genomic DSBs prompted us to examine whether RNF8 is required to initiate a DDR at uncapped telomeres. To examine whether RNF8 is required to localize DDR proteins to dysfunctional telomeres, uncapped telomeres were generated in both *Rnf8* competent and *Rnf8*$^{-/-}$ SV40LT immortalized mouse embryonic fibroblasts (MEFs) by removing mTRF2 with retrovirus-mediated short hairpin RNA against mTRF2 (shTrf2), or by expressing the dominant-negative mutant mTPP1$^{\Delta RD}$ to deplete the endogenous mTPP1-mPOT1a/b

complex[3,4,6,7]. Removal of mTRF2 or mTPP1-mPOT1a/b from *Rnf8*$^{+/+}$ MEFs initiated equally robust DDR at telomeres, manifested as 53BP1 and γ-H2AX positive dysfunctional telomere-induced DNA damage foci (TIFs) (Fig. 1a, b). In *Rnf8*$^{-/-}$ MEFs devoid of mTRF2 or mTPP1-mPOT1a/b, γ-H2AX-positive TIFs, but not ~3BP1-positive TIFs, accumulated on dysfunctional telomeres (Fig. 1a–c). Compared with *Rnf8*$^{+/+}$ MEFs, in *Rnf8*$^{-/-}$ MEFs γ-H2AX-positive TIF formation was reduced ~3-fold at telomeres devoid of either mTRF2 or mTPP1-mPOT1a/b (Fig. 1c). These results suggest that RNF8 is absolutely required for recruitment of 53BP1 to uncapped telomeres. In contrast, RNF8 is required for efficient phosphorylation of γ-H2AX to uncapped telomeres.

We next examined whether RNF8 localizes to uncapped telomeres. RNF8 contains an N-terminal forkhead-associated (FHA) domain which is required for its localization to damaged DNA by interacting with phosphorylated MDC1[12,13,15]. RNF8 also contains a C-terminal RING-finger domain responsible for its ubiquitin ligase activity[16,17]. We found that wild-type FLAG-mRNF8 readily localized to dysfunctional telomeres lacking mTRF2 or mTPP1-mPOT1a/b (Fig. 1d, e, f). Similarly, the mRNF8^{C406S} RING domain mutant also localized to uncapped telomeres (Fig. 1d, e, f). In contrast, the mRNF8^{R42A} FHA domain mutant failed to localize to uncapped telomeres (Fig. 1d, e, f), supporting the notion that this domain is critically important for localization of RNF8 to sites of DNA damage.

Reconstitution of wild-type mRNF8 into *Rnf8*$^{-/-}$ MEFs in the setting of mTPP1-mPOT1a/b deficiency completely restored γ-H2AX-positive TIF formation (Supplementary Fig. 1a, b). Since the mRNF8^{C406S} RING-finger domain mutant readily localizes to uncapped telomeres, we asked whether this domain is required for TIF formation. Reconstitution of *Rnf8*$^{-/-}$ MEFs with the mRNF8^{C406S} mutant failed to bring γ-H2AX-positive TIF levels back to those observed in *Rnf8*$^{-/-}$ MEFs reconstituted with wild-type mRNF8 (Supplementary Fig. 1a, b). Taken together, these results suggest that localization of mRNF8 to uncapped telomeres requires an intact FHA domain. In contrast, the RNF8 E3 ubiquitin ligase function is required for efficient recruitment of DNA damage checkpoint proteins to dysfunctional telomeres.

RNF8 is required for telomere end protection

We asked whether RNF8 is required for the repair of dysfunctional telomeres. We have recently shown that dysfunctional telomeres engage two distinct DNA repair pathways: removal of mTRF2 elicits the classical non-homologous end joining (C-NHEJ) reaction to generate long chains of end-to-end chromosome fusions with robust telomere signals at fusion sites, while removal of mTPP1-mPOT1a/b engages an alternative-NHEJ (A-NHEJ) repair pathway that produces fused chromosome without telomeres at fusion sites[7]. Metaphase spreads of *Rnf8*$^{+/+}$ and *Rnf8*$^{-/-}$ MEFs were generated and telomere-PNA FISH used to examine the status of chromosome ends. While *Rnf8*$^{+/+}$ MEFs displayed only rare p-p arm chromosomal aberrations involving ~6% of all chromosomes examined, *Rnf8*$^{-/-}$ cells displayed elevated spontaneous chromosome aberrations, including p-p fusions, q-q fusions, p-q fusions, rings and tri- or quadri-radials (Fig. 2a, b). A ~20-fold increase in telomere signal-free chromosome ends were observed in metaphases from *Rnf8*$^{-/-}$ MEFs, corresponding to the ~20% decrease in total telomere length revealed by TRF Southern analysis (Fig. 2a, Supplementary Fig. 2a, b). These results suggest that telomere end protection is compromised in the absence of RNF8.

In contrast to the chromosome fusions observed upon mTRF2 depletion, chromosome fusions observed in the setting of mRNF8 deficiency resembled those observed when mTPP1-mPOT1a/b was depleted from telomeres[7]. Indeed, removal of mTPP1-mPOT1a/b from telomeres of *Rnf8*$^{-/-}$ MEFs increased the number of chromosome fusions ~2.5-fold, to involve ~30% of all chromosome ends (Fig. 2c, d). These results suggest that in the absence

of mRNF8, telomeres are rendered dysfunctional and are repaired via the A-NHEJ pathway. To directly assess whether the C-NHEJ repair pathway is functional in the absence of mRNF8, we removed mTRF2 from telomeres of *Rnf8*$^{-/-}$ MEFs. End-to-end chromosome fusions decreased ~10 fold in *Rnf8*$^{-/-}$ MEFs devoid of mTRF2, and characteristic long trains of fused chromosomes with telomeres at fusion sites were not observed (compare Fig. 2e, left and right panels). The small number of chromosome fusions that remain were indistinguishable from those observed upon mTPP1-mPOT1a/b depletion (Fig. 2e, f), suggesting that they too are repaired via ANHEJ. This result suggests that C-NHEJ is abrogated in *Rnf8*$^{-/-}$ MEFs, in agreement with our data demonstrating the inability of 53BP1 to localize to uncapped telomeres in the absence of mRNF8, and the requirement for 53BP1 in promoting C-NHEJ-mediated repair of mTRF2-depleted telomeres[7].

To assess which domains of RNF8 are required to mediate A-NHEJ of uncapped telomeres, we expressed mRNF8 wild-type or the mRNF8^{C406S} RING-finger domain mutant in *Rnf8*$^{-/-}$ MEFs. Reconstitution of *Rnf8*$^{-/-}$ MEFs devoid of mTPP1-mPOT1a/b with wild-type Rnf8, but not with the mRNF8^{C406S} RING domain mutant, reduced the number of chromosome fusions ~6-fold, suggesting that a functional mRNF8 RING domain is required to repress A-NHEJ mediated chromosome fusions (Supplementary Fig. 3a, b). Taken together, our data suggest that the E3 ubiquitin ligase function of mRNF8 is required to repress A-NHEJ at telomeres. In addition, mRNF8 is also required for C-NHEJ-mediated chromosome fusions by recruiting 53BP1 to telomeres devoid of mTRF2.

RNF8 is required for the accumulation of the mTPP1-mPOT1a/b complex at telomeres

The observation that the A-NHEJ pathway is activated at telomeres of *Rnf8*$^{-/-}$ MEFs suggests that the mTPP1-mPOT1a/b complex might be functionally compromised in the absence of mRNF8. We hypothesize that accumulation of mTPP1-mPOT1a/b at telomeres is reduced in *Rnf8*$^{-/-}$ MEFs, resulting in telomere deprotection and failure to repress A-NHEJ-mediated chromosome fusions. In support of this notion, Western analysis revealed that expression of endogenous (Fig. 3a, lanes 1 and 3) and over expressed (lanes 5 and 7) mTPP1 was reduced ~3-fold in *Rnf8*$^{-/-}$ MEFs, while the expression of endogenous mTRF2 was not appreciably affected. To confirm that RNF8 levels influenced endogenous TPP1 protein expression, we depleted *RNF8* in HeLa cells using two independent siRNAs. Endogenous hTPP1 protein levels were markedly reduced in hRNF8-depleted HeLa cells due to a decrease in protein half-life, while hTRF2 protein levels remain unaltered (Fig. 3b and Supplementary Fig. 4a). Since *Tpp1* mRNA levels were unaffected in both *Rnf8*$^{-/-}$ MEFs and in *RNF8* depleted HeLa cells, these results suggest that hRNF8 regulates hTPP1 at the posttranslational level (Supplementary Fig. 4b, c).

We next performed indirect immunofluoresence and telomere-PNA FISH on *Rnf8*$^{+/+}$ and *Rnf8*$^{-/-}$ MEFs to examine the level of endogenous mTPP1 at telomeres. Compared to *Rnf8*$^{+/+}$ MEFs, *Rnf8*$^{-/-}$ MEFs displayed a ~5-fold reduction of endogenous mTPP1 at telomeres (Fig. 3c, d). Examination of epitope-tagged shelterin components revealed that while hTRF1, hTRF2, and hRAP1 were found in similar quantities at telomeres of both *Rnf8*$^{+/+}$ and *Rnf8*$^{-/-}$ MEFs, hTIN2, hTPP1 and mPOT1a accumulation at telomeres were all reduced ~3-fold in *Rnf8*$^{-/-}$ MEFs (Supplementary Fig. 5a–c). This result is in agreement with previous observations that hTPP1 expression is critical for the localization of both hPOT1 and hTIN2 to telomeres[18].

Finally, we asked whether the ubiquitin ligase activity of RNF8 is required for accumulation of TPP1 at telomeres. While expression of wild-type mRNF8 in *Rnf8*$^{-/-}$ MEFs resulted in robust accumulation of mTPP1 at telomeres, the mRNF8^{C406S} RING domain mutant was unable to restore mTPP1 expression at telomeres (Fig. 3e, Supplementary Fig. 6). Taken

together, these results suggest that stable accumulation of mTPP1 at telomeres requires the ubiquitin ligase activity of mRNF8.

Loss of RNF8 results in increased TPP1 turnover by proteasome-mediated degradation

The ubiquitin/26S proteasome pathways are involved in protein degradation. We addressed the possibility that the decreased mTPP1 protein levels observed in *Rnf8*$^{-/-}$ MEFs is due to increased proteasome-mediated turnover of mTPP1. We examined the levels of endogenous mTPP1, as well as exogenously expressed HA-mTPP1, in both *Rnf8*$^{+/+}$ and *Rnf8*$^{-/-}$ MEFs in the presence or absence of the proteasome inhibitor MG132. MG132 treatment substantially increased endogenous mTPP1 protein levels in *Rnf8*$^{-/-}$ MEFs to levels observed in *Rnf8*$^{+/+}$ cells, suggesting that mRNF8 protects mTPP1 from proteasome-dependent degradation (Fig. 4a, b). Exogenously expressed FLAG-hTIN2 was also stabilized by the addition of MG132 in *Rnf8*$^{-/-}$ MEFs, consistent with previous data suggesting that hTPP1 stabilizes hTIN2 at telomeres[18]. (Fig. 4c). In contrast, the addition of MG132 did not substantially influence the exogenous expression of FLAG -hTRF1, FLAG -hTRF2, HA-hRAP1 and Myc-mPOT1a in *Rnf8*$^{-/-}$ MEFs (Fig. 4c, d). Since MG132 treatment stabilized mTPP1 protein levels in the absence of RNF8, we next asked whether stabilized mTPP1 are observed at telomeres of *Rnf8*$^{-/-}$ MEFs treated with MG132. While treatment with MG132 resulted in rapid depletion of the nuclear ubiquitin pool in IR-treated HeLa cells[15], the absence of exogenous DNA damaging agents resulted in the slow depletion of the nuclear ubiquitin pool from MG132-treated *Rnf8*$^{+/+}$ MEFs, resulting in the retention of the majority of conjugated ubiquitin in the nucleus and mTPP1 at telomeres (Fig. 4e, f, Supplementary Fig. 7a, b). Surprisingly, both endogenous and exogenously expressed mTPP1 were unable to localize to telomeres in *Rnf8*$^{-/-}$ MEFs treated with MG132, instead displaying diffuse cytoplasmic staining (Fig. 4e, f). Taken together, these results suggest that functional RNF8 is required for TPP1 to localize to telomeres and for the maintenance of TPP1 protein stability by preventing its proteosome-mediated degradation in the cytoplasm.

Physical interaction between RNF8 and TPP1 stabilizes TPP1 through ubiquitylation

To determine the mechanism through which RNF8 regulates TPP1 stability, we asked whether RNF8 physically interacts with TPP1. We co-transfected 293T cells with either FLAG-mRNF8 and HA-hTPP1 or HA-mRNF8 and Myc-hTPP1. Whole-cell extracts were subjected to reciprocal immunoprecipitation with anti-HA antibody. FLAG-mRNF8 was found to co-precipitate with HA-hTPP1, while Myc-hTPP1 associated with HA-mRNF8, suggesting a specific interaction between RNF8 and TPP1 *in vivo* (Fig. 5a, Supplementary Fig. 8). The finding that TPP1 interacts physically with RNF8 led us to hypothesize that RNF8 might mediate TPP1 ubiquitylation. To examine whether TPP1 ubiquitylation is directly and specifically mediated by RNF8, we carried out an *in vitro* ubiquitylation assay with purified wild type mRNF8 and the catalytic dead mRNF8^{C406S} RING domain mutant in presence of purified E1 ubiquitin-activating enzyme (Uba1) and its E2 (Ubc13 and Mms2) together with ATP ubiquitin[19,20]. Western blotting with anti-mTPP1 and anti-HA antibodies suggests that RNF8 polyubiquitylates TPP1 in an ATP-dependent manner (Fig. 5b). In contrast, the mRNF8^{C406S} mutant failed to ubiquitylate mTPP1, suggesting that the RNF8 RING domain is essential for TPP1 ubiquitylation (Fig. 5b; compare lanes 1 and 4). Omission of any component required for ubiquitin conjugation completely abrogates TPP1 ubiquitylation (Fig. 5b and data not shown). The mRNF8^{C406S} mutation did not alter the ability of mRNF8^{C406S} to bind to mTPP1 (data not shown). Collectively, these results suggest that RNF8 directly and specifically ubiquitylate TPP1 through its E3 ligase function.

TPP1 ubiquitylation by RNF8 was further validated by an *in vivo* ubiquitylation assay using a HeLa-His/biotin-ubiquitin (HeLa UB) cell line stably expressing tandem 6× His-biotin-

tagged ubiquitin[21]. This system offers the advantage of purifying ubiquitylated proteins under fully denatured conditions, thus reducing non-specific interactions. In order to perform this assay, we stably expressed HA-mTPP1 in HeLa UB cell lines and treated the cells with biotin overnight. Ubiquitylated protein was then purified with strepavidin-agarose beads. Several HA-positive bands were observed, were observed, S.</author></authors></ contributors><auth-address>D**epartme**nt of Genetics, MD Anderson Cancific, since they were not detected in the absence of His-biotin-tagged ubiquitin expression or in HeLa UB cell lines transfected with empty vector (Fig. 5c). As further proof of specificity, we treated HeLa UB cells stably expressing mTPP1 with a shRNA against mTPP1. mTPP1 polyubiquitylation was undetectable in mTPP1 depleted cells, demonstrating the specificity of mTPP1 polyubiquitylation *in vivo* (Fig. 5c, lane 4).

Ubiquitin can form polymers *in vivo* through any of its seven lysyl residues[22]. To analyze the class of polyubiquitin chains supported by RNF8's E3 ligase activity on TPP1, we co-transfected HeLa cells with plasmids encoding HA-mTPP1 and His-tagged expression vectors for ubiquitin species in which all lysines were mutated to arginines except the ones indicated. This system enables the *in vivo* synthesis of polyubiquitin chains containing defined isopeptide linkages. The expressed His-tagged ubiquitin was then pulled down from the cell lysates with Ni^{2+}-NTA agarose beads under denatured conditions. Subsequent anti-HA immunoblotting enabled detection of ubiquitylated HA-mTPP1. We found that wild-type mTPP1 undergoes ubiquitylation with both lysine 48 and lysine 63 linked polyubiquitin chains (Fig. 5d, lanes 3, 5, 6). Other polyubiquitin chains, including K6, K11, K27, K29, and K33 were not conjugated to mTPP1 (see below). We next asked if the K63 and K48 polyubiquitin chains on mTPP1 were specifically generated by endogenous hRNF8. To accomplish this, we transfected HeLa cells with His-tagged K48 and K63 ubiquitin species and treated them with siRNA against *RNF8.* Both K48 and K63 polyubiquitin chains were completely abolished in hRNF8-depleted HeLa cells (Fig. 5d, lanes 7, 8). In addition, treatment with MG132 in HeLa cells depleted of endogenous hRNF8 restored K48 but not K63 polyubiquitin chains on mTPP1 (Supplementary Fig. 9, lanes 8, 9). Therefore, our data suggest that TPP1 can be ubiquitylated by RNF8 through K63 polyubiquitin chain, while K48 polyubiquitin chains of TPP1 are likely synthesized by an unknown ubiquitin ligase.

To further examine the role of RNF8-mediated K63 polyubiquitin on TPP1 stability and telomere metabolism, we probed immunoprecipitated nuclear and cytoplasmic extracts isolated from $Rnf8^{+/+}$ or $Rnf8^{-/-}$ MEFs expressing mTPP1 with linkage-specific antibodies that specifically discriminate ubiquitin chains formed by either K63 or K48[23]. mTPP1 ubiquitylated species were only detected by the anti- K63 but not with the anti-K48-linkage antibody in the nuclear fraction isolated from $Rnf8^{+/+}$ MEFs (Supplementary Fig. 10a, b). The presence of K63-linked ubiquitin chains was not detected in $Rnf8^{-/-}$ MEFs, strongly suggesting that RNF8 is required to generate K63 chain on TPP1(Supplementary Fig. 10a, b).

Finally, we utilized a RNF8 RING domain mutant ($hRNF8^{I405A}$) specifically impaired to perform K48-based but not K63-based polyubiquitylation reaction[24]. In contrast to the $hRNF8^{\Delta RING}$ or the $mRNF8\ RING^{R42A}$ mutants, $hRNF8^{I405A}$ efficiently targeted mTPP1 to telomeres in $Rnf8^{-/-}$ MEFs (Supplementary Fig. 11). Reconstitution of $hRNF8^{I405A}$ into $Rnf8^{-/-}$ MEFs in the setting of mTRF2 deficiency completely restored 53BP1-positive TIF formation (Supplementary Fig. 12a) and C-NHEJ-mediated end-to-end chromosome fusions (Supplementary Fig. 12b, c). Taken together, these results suggest that RNF8-dependent K63-linked, but not K48-linked ubiquitin chain formation on TPP1 is required to promote TPP1 stability and function at telomeres.

RNF8 can accommodate on its RING finger domain with several E2 enzymes to synthesize either K48 or K63 polyubiquitin chains on its substrates[16]. UBC13 is the E2 conjugating enzyme that exclusively promotes K63 linked ubiquitylation[25,26]. Our data suggest that RNF8 can promote *in vivo* synthesis of K63, but not K48 polyubiquitin chain on TPP1 (Figure 5d, Supplementary Figure 9). Therefore, we hypothesized that RNF8 physically interacts with UBC13 to generate K63-linked polyubiquitin chains to stabilize TPP1 and prevent its degradation. To support our hypothesis, we performed *in vitro* ubiquitylation assays with purified hTPP1, hRNF8, Ubc13, Mms2, Uba1 along with wild type or mutant ubiquitins. Both the wild type and the K63 ubiquitins were efficiently conjugated to hTPP1, suggesting that the K63 isopeptides is the preferred linkage for hTPP1 ubiquitylation by hRNF8 together with UBC13 (Fig. 5e). To further confirm that K63 ubiquitylation of hTPP1 is dependent upon UBC13, we used three different siRNA to knockdown UBC13. As expected, knockdown of UBC13 resulted in the loss of hTPP1 expression, further solidify the notion that hRNF8 coordinates with UBC13 to conjugate K63 polyubiquitin chains on hTPP1 to prevent its degradation (Supplementary Fig. 13).

A conserved lysine 233 residue of TPP1 is required for RNF8-mediated TPP1 ubiquitylation and localization to telomeres

Our data demonstrate that RNF8 directly ubiquitylates and stabilizes TPP1 at telomeres. We next sought to determine the lysine residues critical for TPP1 ubiquitylation and its localization to telomeres. Alignment of TPP1 sequences across several vertebrate species revealed three highly conserved lysine residues: $TPP1^{K170}$, $TPP1^{K232}$ and $TPP1^{K233}$ all reside within the OB fold, while $TPP1^{K467}$ resides in the S/T domain (Fig. 6a). To test the roles of these lysine residues on hTPP1 ubiquitylation, we mutated them individually or together into arginines and trasfected these FLAG-hTPP1 mutants into HeLa cells for *in vivo* ubiquitylation assays. We also generated purified mutant TPP1 proteins for *in vitro* ubiquitylation assays. All mutants expressed at similar levels in HeLa cells, suggesting that lysine to arginine mutations did not impact upon protein stability (Supplementary Fig. 14a, lower panel). Western analysis revealed that mRNF8-mediated hTPP1 *in vitro* ubiquitylation was reduced ~2.5-fold in the $hTPP1^{K233R}$ mutant as compared to $hTPP1^{FL}$ (Fig. 6b). Analysis of the $hTPP1^{K232R,K233R}$ double mutant revealed that it is completely unable to be ubiquitylated *in vivo* (Supplementary Fig. 14a, upper panel). In contrast, $hTPP1^{K170R}$ and $hTPP1^{K476R}$ mutants did not alter mRNF8-mediated hTPP1 ubiquitylation, while uqiquylation was only slightly reduced in the $hTPP1^{K232R}$ mutant. These results suggest that lysine 233 is required for mRNF8-mediated ubiquitylation.

Since the ubiquitylation status of TPP1 might influence its localization to telomeres, we examined the telomere localization of the hTPP1 lysine mutants. FLAG-$hTPP1^{WT}$, FLAG-$hTPP1^{K170R}$, FLAG-$hTPP1^{K232R}$ and FLAG-$hTPP1^{K476R}$ were all visualized on telomeres (Fig. 6c, d). In contrast, MEFs transfected with FLAG-$TPP1^{K233R}$ and the double mutant FLAG-$hTPP1^{K232R/K232R}$ displayed only diffused nuclear staining, again reinforcing the observation that lysine K233 is the critical lysine residue for the accumulation of TPP1 at telomeres (Fig. 6c, d). The failure of the FLAG-$hTPP1^{K233R}$ mutant to localize to telomeres suggests that failure to ubiquitylate TPP1 at lysine 233 results in either an inability of this mutant to be recruited to telomeres, or an inability to be retained there. Retention of endogenous TPP1 at telomeres requires the presence of nuclear ubiquitin, since the addition of MG132 depletes TPP1 from telomeres (Supplemental Fig. 7a, b). This result suggests that ubiquitylation of TPP1 by RNF8 is important for its retention at telomeres.

Since POT1 recruitment to telomeres depends upon its interaction with TPP1[3,27,28], we next asked whether localization of POT1-TPP1 complex to telomeres requires TPP1 ubiquitylation. To address this question, we co-transfected Myc-mPOT1a with either FLAG-$hTPP1^{WT}$ or FLAG-tagged hTPP1 mutants into wild-type MEFs. Myc-mPOT1a failed to

localize to telomeres only in the presence of FLAG-hTPP1^{K233R} (Supplementary Fig. 14b and data not shown). Co-IP experiments revealed that all hTPP1 mutants were able to interact efficiently to mPOT1a *in vitro* (Supplementary Fig. 14c). Metaphases isolated from wild-type MEFs expressing hTPP1^{K233R} also displayed ~3-fold increase in chromosome fusions, likely due to its ability to titrate endogenous mPOT1a/b away from telomeres (Supplementary Fig. 14d). These results suggest that retention of the POT1-TPP1 complex at telomeres requires RNF8-mediated ubiquitylation of TPP1 at lysine 233.

Discussion

In this study, we reveal an unexpected link between the E3 ubiquitin ligase RNF8 and maintenance of telomere function. We show that the stability of the shelterin component TPP1 at telomeres is controlled by RNF8. RNF8 binds directly to TPP1 and catalyses the formation of K63 polyubiquitin chains on TPP1. In the absence of RNF8, endogenous TPP1 levels are markedly reduced, likely through the K48 polyubiquitin-mediated proteolysis via the 26S proteasome, resulting in telomere dysfunction and A-NHEJ-mediated chromosome fusions. The stability of TPP1 is dependent upon the addition of RNF8-mediated K63 polyubiquitin chains, since TPP1 remained stable in the setting of a RNF8 mutant that was specifically unable to catalyze K48-linked ubiquitin chain formation. We also found that RNF8 cooperates with UBC13 to catalyze the formation of UbK63 chains at least on the lysyl 233 residue of TPP1. Since the formation of UbK63 chains is involved in DNA repair reactions and not in proteasomal degradation[29], our data suggest that in addition to the recruitment of DNA damage response factors to ubiquitinated histones, RNF8-mediated ubiquitylation of TPP1 impacts upon DNA damage signaling and repair reactions at telomeres.

Post-translational modifications appear to be an evolutionarily conserved mechanism to modulate telomere stability. In human cells, TRF1 is poly (ADP-ribosyl)ated by tankyrase 1, leading to its release from telomere and its subsequent ubiquitylation by SCF^{Fbx4} and degradation by the proteasome[30–34]. TIN2 suppress TRF1 polyubiquitylation by sequestering its degradation motif from recognition by SCF^{Fbx4} [32]. The p53-dependent ubiquitylation of TRF2 by the E3 ligase Siah1 impacts upon the onset of cellular senescence [35]. While these studies document the importance of ubiquitin-mediated proteolysis of shelterin components for telomere maintenance, our studies reveal that RNF8-mediated ubiquitylation is required to stabilize TPP1 at telomeres. The TPP1-POT1 complex plays an important role to repress the DDR pathway at telomeres. Removal of TPP1-POT1 from telomeres increases the abundance of the single-stranded telomere overhang, resulting in the recruitment of RPA and activation of Chk1 phosphorylation[36]. These results demonstrate that this complex is essential for the repression of ATR signaling[4–6,28,37]. In addition, this complex also guards against the activation of an A-NHEJ-dependent repair pathway, leading to end-to-end chromosome fusions[7]. In contrast to TPP1-POT1, removal of TRF2 from telomeres activates ATM signaling and chromosome fusions that are repaired via the 53BP1-dependent C-NHEJ pathway[7]. Since recruitment of 53BP1 to DNA damage repair sites requires RNF8, our studies suggest a scenario in which RNF8 controls both C-NHEJ and A-NHEJ-mediated repairs at telomeres (Supplemental Figure 15). We speculate that in the presence of RNF8, TPP1 level at telomere is stabilized by the formation of Ub K63 chains, repressing A-NHEJ while favoring C-NHEJ mediated repair. In the setting of RNF8 deficiency, a reduction in TPP1 levels at telomeres favors A-NHEJ, while C-NHEJ-mediated repair is abolished.

Disregulation of E3 ligases have been shown to promote chromosome instability and increased cancer risk, largely due to the increased stability of oncoproteins or enhanced degradation of tumor suppressors[38–40]. Interestingly, *Rnf8*$^{-/-}$ mice exhibit increased

genomic instability and increased cancer incidence, suggesting that RNF8 is a novel tumor suppressor[41]. Along this line, it is worth noting that decreased TPP1 protein levels has been observed in patients with CLL[42] in agreement with observations that mice deficient in TPP1 exhibit increased genomic instability and increased tumorigenesis in the setting of p53 deficiency[43]. The identification of TPP1 as a substrate of RNF8 suggests that an important physiological function of RNF8 is to maintain telomere integrity by promoting the stability of TPP1.

Experimental procedures

Materials and Methods

Antibodies—A polyclonal antibody against human 53BP1 and RNF8 has been previously described[12,44]. Anti γ-H2AX and anti-hTRF2 was from Upstate. Anti-Myc was obtained from Santa Cruz. Anti-FLAG, Anti-HA and Anti-γ-tubulin (clone GTU-488) were purchased from Sigma. Anti mouse antibodies against mTRF1 and mTRF2 was a kind gift from Dr. Jan Karlseder, Salk Institute. Anti-mTPP1 antibody was generated using the following peptide sequence: CSQLLDEVREDQDHR. Anti-hTPP1 was a generous gift from Dr. Zhou Songyang, Baylor College of Medicine. Anti-hRAP1 and anti-hUBC13 antibodies were purchased from Bethyl laboratories and Calbiochem respectively. Anti-ubiquitylated protein, clone FK2 was obtained from Millipore. The linkage-specific antibodies to K63 (Apu3.A8) and K48 (Apu2.07) ubiquitin conjugates were provided by Vishva M. Dixit (Genentech).

Vectors, shRNA and siRNA—Full-length mRNF8, mRNF8 points mutants[13], mTPP1 and mPOT1a cDNAs were cloned into pQCXIP-puro retroviral expression vectors. All the constructs were confirmed by sequencing. hRNF8 was as described[12]. hTRF1, hTRF2, hTIN2, hTPP1 were as described[18]. pLPC-hRAP1 was from Dr. Ming Lei, University of Michigan. Wild-type ubiquitin and ubiquitin mutants are generated by the Jin lab (Li and Jin, unpublished). Lysine to arginine point mutations in hTPP1 were introduced using side-directed mutagenesis according to manufacturer's protocol (Stratagene). mTRF2 shRNA, mTPP1 shRNA and mTPP1$^{\Delta RD}$ were as described[4,6]. siRNAs against hRNF8 was purchased from Invitrogen.

Generation of *Rnf8*$^{-/-}$ mouse and MEFs—*Rnf8* knock-out mice have been previously described[41]. *Rnf8*$^{-/-}$ MEFs from E13.5 day embryos were isolated, genotyped and immortalized at passage 2 using pBabe-SV40^{LT}.

Culture of MEFs and retroviral infection: *Rnf8* wild-type and null MEFs were cultured in DMEM supplemented with 10% FCS and maintained in 5% CO2 at 37°C. For viral particle packaging, 293T cells were transiently transfected with pCL Eco using Lipofectamine Plus (Invitrogen) following the manufacturer's protocols. Viral supernatants collected 48–72 hours post-transfection were filtered through 0.45um membranes and directly used to infect the *Rnf8*$^{+/+}$and *Rnf8*$^{-/-}$ MEFs, with two consecutive retroviral infections at 12 h intervals. After 120h of the second infection, stable pool of cells were selected in 2μg/ml puromycin and harvested for PNA-telomere FISH and CO-FISH analysis.

Immunofluorescence and telomere dysfunction- induced foci analysis:
Immunofluorescence -Telomere PNA FISH was performed as described[45]. After 72 hours of retroviral infection with Trf2 shRNA or mTPP1$^{\Delta RD}$, cells grown on cover slips were fixed for 10 min in 2% sucrose/2% paraformaldehyde at RT followed by PBS washes. Cover slips were blocked for one hour in blocking solution (0.2% fish gelatin, 0.5% BSA in 1XPBS). The cells were incubated with primary antibody for 2 hour at RT. After PBS washes,

coverslips were incubated with the appropriate secondary antibodies for one hour followed by washes in PBS. Next, the cover slips were fixed with 4% paraformaldehyde for 10 min at RT and washed extensively in PBS. Hybridizing mix (70 % formamide, 2% BSA, 100ug/ml tRNA) containing peptide- nucleic acid (PNA) 5'-Tam-OO-$(CCCTAA)_4$-3' probe (Applied Biosystem) was added to each cover slip and the cells were denatured by heating for 3 min at 80°C on a heat block. After 2 hour incubation at RT in the dark, cells were washed twice with 70 % formamide/ 0.1% Tween 20/ 0.1% BSA/ 10 mM Tris-HCl, pH 7.5 followed by 3 washes in 50mM Tris-HCl, pH 7.5/150 mM NaCl/ 0.1% BSA/ 0.1% Tween-20. DNA was counterstained with DAPI. A minimum of 100 cells with greater than four 53BP1 or γ-H2AX signals co localized with telomere signals were captured with an Andor CCD camera on a Nikon Eclipse 800 microscope.

Telomere PNA-FISH analysis: Metaphase chromosomes from MEFs were prepared as previously described previously[4,6,37,46]. Chromosomes were fixed and telomere-FISH with peptide- nucleic acid (PNA) Tam-OO-$(CCCTAA)_4$- probe (Applied Biosystem) was performed as described previously[36]. Images were captured with an Andor CCD camera on a Nikon Eclipse 800 microscope and processed with Nikon Imaging software.

Telomere Length and G-Strand Overhang Assays: For in-gel detection of telomere length and G-stand overhang, a total of 2×10^6 cells were subjected to pulse-field electrophoresis. Subsequent denaturation and hybridization with ^{32}P-labeled T_2AG_3 oligonucleotides were performed as described previously[4].

Immunoprecipitation: 293T cells grown in 6 well plates were co-transfected with hTPP1 and mRNF8 encoding plasmids or vector control. 72 hours after transfection, cells were harvested in lysis buffer containing 50mM Tris (pH7.5), 150mM NaCl, 0.5% NP-40, 0.2mM DTT, 10 mM β-glycerol phosphate, 10 mM *p*-nitro phenyl phosphate, 0.1 μM okadaic acid, and 5 mM NaF. Extracts were subjected to immunoprecipitation with anti-HA agarose beads (Sigma) followed with SDS-PAGE and western blotting with indicated antibodies. Nuclear and cytoplasmic extracts from HeLa cells used for immunoprecipitation were prepared using the NE-PER nuclear protein extraction kit (Pierce).

In *vitro* ubiquitylation assays: The hTPP1 ubiquitylation assay was performed based on a protocol described previously[19]. Briefly, hTPP1 (50ng) was incubated with ubiquitin-activating enzyme (E1, 50ng), MMS2 and Ubc13 (100ng each), RNF8 (100ng), ubiquitin (1μg), ubiquitin aldehyde (1μM) and ATP at 30°C for 30 min. hTPP1 was purified from 293T cells transfected with the encoding plasmid. E1 and RNF8 were purified from insect cells, Sf9, infected by recombinant baculoviruses and Mms2 and Ubc13 were purified from bacteria. Ubiquitin and ubiquitin aldehyde were purchased from Boston Biochem. In some experiment, lysine mutant ubiquitin was used to determine the chain linkage.

In *vivo* protein ubiquitylation assay: His-Biotin-Ubiquitin HeLa cells grown in 10% FBS and 0.5μg Balsticidin were infected with empty pQCXIP vector, HA-mTPP1 or co-transfect with both HA-mTPP1 and shTpp1. Stably infected cells were incubated with 2μg/ml biotin overnight. Cells were harvested in lysis buffer containing 100mM Tris-HCl (pH 8.0), 200mM NaCl, 8M Urea, 0.2%SDS, sonicated and incubate with 5μl strepavidin-agarose slurry at room temperature overnight. Washed beads with 1.0 ml of lysis buffer thrice at 7000 rpm for 5 minutes, subjected to SDS-PAGE and Western blotting with the indicated antibodies.

In *vivo* ubiquitylation assay using nickel-NTA-agarose purification: In *vivo* ubiquitylation using nickel-NTA-agarose in HeLa cells was performed as described

earlier[47]. Transfected cells were lysed in 1 ml of buffer A (6 M guanidinium-HCl/0.1 M Na2HPO4/NaH2PO4, pH 8.0/10 mM imidazole) per 100-mm dish 24 hr after removal of the precipitate. The lysate was sonicated for 30 sec to reduce viscosity and then mixed on a rotator with 50 μl (settled volume) of nickel-NTA-agarose (Qiagen) for 3 hr at room temperature. The beads were washed three times with 1 ml of buffer A, twice with 1 ml of buffer A diluted in 25mM with Tris-HCl (pH 6.8)/20 mM imidazole 1:4, and twice with 1 ml of 25mM Tris-HCl (pH 6.8)/20 mM imidazole. Purified proteins eluted by boiling the beads in 2× sample buffer supplemented with 200 mM imidazole subjected to SDS-PAGE and immunoblotting.

Supplementary Material

Refer to Web version on PubMed Central for supplementary material.

Acknowledgments

We are grateful to Dr. Jan Karlseder for providing anti-mouse TRF1 and TRF2 antibodies, to Dr. Zhou Songyang for providing anti-human TPP1 antibody and TPP1 cDNA constructs and to Dr. Daniel Durocher for providing mouse RNF8 and RNF8 mutant cDNAs. We would like to thank Dr. Asha Multani for help with chromosome analysis and Mr. Ilyas Patanam for technical support.

References

1. de Lange T. How Shelterin Solves the Telomere End-Protection Problem. Cold Spring Harb Symp Quant Biol. 2011
2. Wang F, et al. The POT1-TPP1 telomere complex is a telomerase processivity factor. Nature. 2007; 445:506–10. [PubMed: 17237768]
3. Xin H, et al. TPP1 is a homologue of ciliate TEBP-beta and interacts with POT1 to recruit telomerase. Nature. 2007; 445:559–62. [PubMed: 17237767]
4. Deng Y, Guo X, Ferguson DO, Chang S. Multiple roles for MRE11 at uncapped telomeres. Nature. 2009; 460:914–8. [PubMed: 19633651]
5. Denchi EL, de Lange T. Protection of telomeres through independent control of ATM and ATR by TRF2 and POT1. Nature. 2007; 448:1068–71. [PubMed: 17687332]
6. Guo X, et al. Dysfunctional telomeres activate an ATM-ATR-dependent DNA damage response to suppress tumorigenesis. Embo J. 2007; 26:4709–19. [PubMed: 17948054]
7. Rai R, et al. The function of classical and alternative non-homologous end-joining pathways in the fusion of dysfunctional telomeres. EMBO J. 2010; 29:2598–610. [PubMed: 20588252]
8. Guirouilh-Barbat J, Rass E, Plo I, Bertrand P, Lopez BS. Defects in XRCC4 and KU80 differentially affect the joining of distal nonhomologous ends. Proc Natl Acad Sci U S A. 2007; 104:20902–7. [PubMed: 18093953]
9. Weinstock DM, Brunet E, Jasin M. Formation of NHEJ-derived reciprocal chromosomal translocations does not require Ku70. Nat Cell Biol. 2007; 9:978–81. [PubMed: 17643113]
10. Harper JW, Elledge SJ. The DNA damage response: ten years after. Mol Cell. 2007; 28:739–45. [PubMed: 18082599]
11. Al-Hakim A, et al. The ubiquitous role of ubiquitin in the DNA damage response. DNA Repair (Amst). 2010; 9:1229–40. [PubMed: 21056014]
12. Huen MS, et al. RNF8 transduces the DNA-damage signal via histone ubiquitylation and checkpoint protein assembly. Cell. 2007; 131:901–14. [PubMed: 18001825]
13. Kolas NK, et al. Orchestration of the DNA-damage response by the RNF8 ubiquitin ligase. Science. 2007; 318:1637–40. [PubMed: 18006705]
14. Wang B, Elledge SJ. Ubc13/Rnf8 ubiquitin ligases control foci formation of the Rap80/Abraxas/Brca1/Brcc36 complex in response to DNA damage. Proc Natl Acad Sci U S A. 2007; 104:20759–63. [PubMed: 18077395]

15. Mailand N, et al. RNF8 ubiquitylates histones at DNA double-strand breaks and promotes assembly of repair proteins. Cell. 2007; 131:887–900. [PubMed: 18001824]
16. Plans V, et al. The RING finger protein RNF8 recruits UBC13 for lysine 63-based self polyubiquitylation. J Cell Biochem. 2006; 97:572–82. [PubMed: 16215985]
17. Ito K, et al. N-Terminally extended human ubiquitin-conjugating enzymes (E2s) mediate the ubiquitination of RING-finger proteins, ARA54 and RNF8. Eur J Biochem. 2001; 268:2725–32. [PubMed: 11322894]
18. O'Connor MS, Safari A, Xin H, Liu D, Songyang Z. A critical role for TPP1 and TIN2 interaction in high-order telomeric complex assembly. Proc Natl Acad Sci U S A. 2006; 103:11874–9. [PubMed: 16880378]
19. Jin J, et al. SCFbeta-TRCP links Chk1 signaling to degradation of the Cdc25A protein phosphatase. Genes Dev. 2003; 17:3062–74. [PubMed: 14681206]
20. Jin J, Li X, Gygi SP, Harper JW. Dual E1 activation systems for ubiquitin differentially regulate E2 enzyme charging. Nature. 2007; 447:1135–8. [PubMed: 17597759]
21. Centore RC, et al. CRL4(Cdt2)-mediated destruction of the histone methyltransferase Set8 prevents premature chromatin compaction in S phase. Mol Cell. 2011; 40:22–33. [PubMed: 20932472]
22. Peng J, et al. A proteomics approach to understanding protein ubiquitination. Nat Biotechnol. 2003; 21:921–6. [PubMed: 12872131]
23. Newton K, et al. Ubiquitin chain editing revealed by polyubiquitin linkage-specific antibodies. Cell. 2008; 134:668–78. [PubMed: 18724939]
24. Lok GT, Dong SS, Thomson TM, Huen MS. Differential Regulation of RNF8-mediated Lys48-and Lys63 based Poly-Ubiquitylation. Nucleic Acid Research. 2011
25. Sobhian B, et al. RAP80 targets BRCA1 to specific ubiquitin structures at DNA damage sites. Science. 2007; 316:1198–202. [PubMed: 17525341]
26. Zhao GY, et al. A critical role for the ubiquitin-conjugating enzyme Ubc13 in initiating homologous recombination. Mol Cell. 2007; 25:663–75. [PubMed: 17349954]
27. Hockemeyer D, et al. Telomere protection by mammalian Pot1 requires interaction with Tpp1. Nat Struct Mol Biol. 2007; 14:754–61. [PubMed: 17632522]
28. Kibe T, Osawa GA, Keegan CE, de Lange T. Telomere protection by TPP1 is mediated by POT1a and POT1b. Mol Cell Biol. 2009; 30:1059–66. [PubMed: 19995905]
29. Huang TT, D'Andrea AD. Regulation of DNA repair by ubiquitylation. Nat Rev Mol Cell Biol. 2006; 7:323–34. [PubMed: 16633336]
30. Chang W, Dynek JN, Smith S. TRF1 is degraded by ubiquitin-mediated proteolysis after release from telomeres. Genes Dev. 2003; 17:1328–33. [PubMed: 12782650]
31. Atanassov BS, et al. Gcn5 and SAGA regulate shelterin protein turnover and telomere maintenance. Mol Cell. 2009; 35:352–64. [PubMed: 19683498]
32. Zeng Z, et al. Structural basis of selective ubiquitination of TRF1 by SCFFbx4. Dev Cell. 2010; 18:214–25. [PubMed: 20159592]
33. Her YR, Chung IK. Ubiquitin Ligase RLIM Modulates Telomere Length Homeostasis through a Proteolysis of TRF1. J Biol Chem. 2009; 284:8557–66. [PubMed: 19164295]
34. Lee TH, Perrem K, Harper JW, Lu KP, Zhou XZ. The F-box protein FBX4 targets PIN2/TRF1 for ubiquitin-mediated degradation and regulates telomere maintenance. J Biol Chem. 2006; 281:759–68. [PubMed: 16275645]
35. Fujita K, et al. Positive feedback between p53 and TRF2 during telomere-damage signalling and cellular senescence. Nat Cell Biol. 2010; 12:1205–12. [PubMed: 21057505]
36. Flynn RL, et al. TERRA and hnRNPA1 orchestrate an RPA-to-POT1 switch on telomeric single-stranded DNA. Nature. 2011; 471:532–6. [PubMed: 21399625]
37. Wu L, et al. Pot1 deficiency initiates DNA damage checkpoint activation and aberrant homologous recombination at telomeres. Cell. 2006; 126:49–62. [PubMed: 16839876]
38. Hoeller D, Hecker CM, Dikic I. Ubiquitin and ubiquitin-like proteins in cancer pathogenesis. Nat Rev Cancer. 2006; 6:776–88. [PubMed: 16990855]

39. Bernassola F, Karin M, Ciechanover A, Melino G. The HECT family of E3 ubiquitin ligases: multiple players in cancer development. Cancer Cell. 2008; 14:10–21. [PubMed: 18598940]
40. Nakayama KI, Nakayama K. Ubiquitin ligases: cell-cycle control and cancer. Nat Rev Cancer. 2006; 6:369–81. [PubMed: 16633365]
41. Li L, et al. Rnf8 deficiency impairs class switch recombination, spermatogenesis, and genomic integrity and predisposes for cancer. J Exp Med. 2010; 207:983–97. [PubMed: 20385750]
42. Augereau A, et al. Telomeric damage in early stage of chronic lymphocytic leukemia correlates with shelterin dysregulation. Blood. 2011
43. Else T, et al. Tpp1/Acd maintains genomic stability through a complex role in telomere protection. Chromosome Res. 2007; 15:1001–13. [PubMed: 18185984]
44. Morales JC, et al. Role for the BRCA1 C-terminal repeats (BRCT) protein 53BP1 in maintaining genomic stability. J Biol Chem. 2003; 278:14971–7. [PubMed: 12578828]
45. Rai R, Chang S. Probing the Telomere Damage Response. Methods Mol Biol. 2011; 735:145–150. [PubMed: 21461819]
46. Multani AS, Chang S. Cytogenetic Analysis of Telomere Dysfunction. Methods Mol Biol. 2011; 735:139–143. [PubMed: 21461818]
47. Campanero MR, Flemington EK. Regulation of E2F through ubiquitin-proteasome-dependent degradation: stabilization by the pRB tumor suppressor protein. Proc Natl Acad Sci U S A. 1997; 94:2221–6. [PubMed: 9122175]

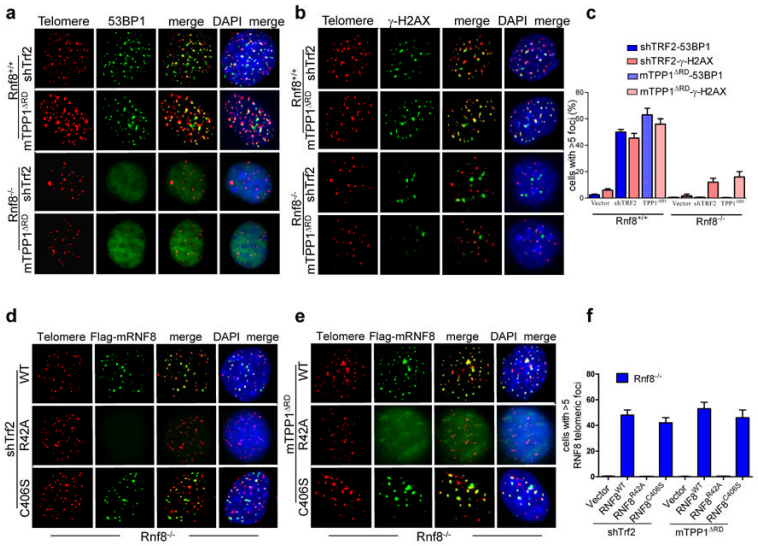

Figure 1. RNF8 is required for the accumulation of DNA damage response factors to dysfunctional telomeres

(a) 53BP1 and **(b)** γ-H2AX positive TIFs in *Rnf8*$^{+/+}$ and *Rnf8*$^{-/-}$ MEFs after depletion of *Trf2* or mTPP1. Cells fixed after 72 hours stained with anti-53BP1 antibody (green) or anti γ-H2AX antibody (green), with Tam-OO-$(CCCTAA)_4$ telomere peptide nucleic acid (red) and 4,6-diamidino-2-phenylindole (DAPI; blue). **(c)** Quantification of 53BP1 and γ-H2AX positive TIFs. A minimum of 100 cells were examined and cells with >4 TIFs were scored as TIF positive. Mean values were derived from at least three experiments. Error bars: s.d. Rnf8 positive foci in *Rnf8*$^{-/-}$ MEFs reconstituted with wild-type mRNF8 and indicated mRNF8 point mutants, followed by **(d)** depletion of *Trf2* or **(e)** mTPP1. Cells were fixed, stained with anti-FLAG antibody (green), Tam-OO-$(CCCTAA)_4$ telomere peptide nucleic acid (red) and DAPI (blue). **(f)** Quantification of mRNF8-positive foci observed in **(d** and **e)**. A minimum of 100 cells were examined and cells with >4 TIFs were scored as TIF positive. Mean values were derived from at least three experiments. Error bars: s.d.

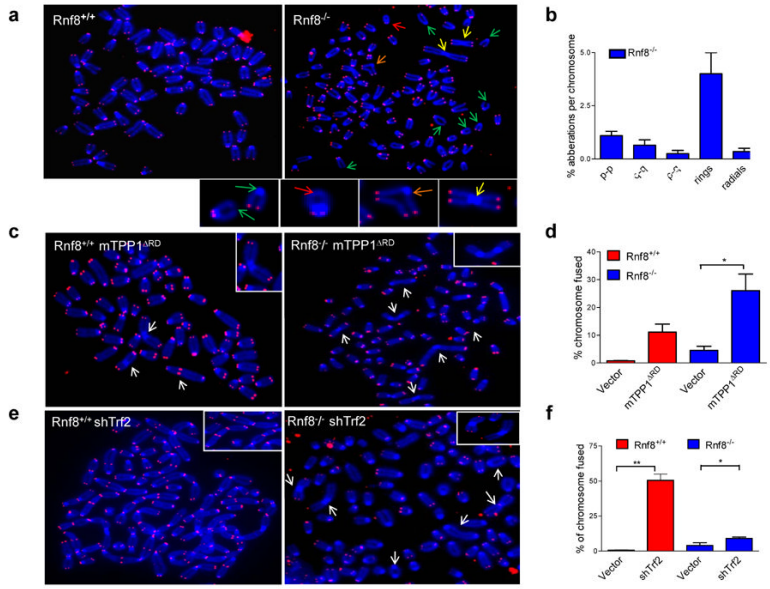

Figure 2. RNF8 is required to protect telomere ends from chromosome aberrations

(a) Telomere-FISH analysis on metaphase chromosome spreads of immortalized *Rnf8*$^{+/+}$ and *Rnf8*$^{-/-}$ MEFs using Tam-OO-(CCCTAA)$_4$ telomere peptide nucleic acid (red) and DAPI (blue). A minimum of 30 metaphases were analyzed per genotype. Red arrows-ring chromosomes; orange arrows: radial chromosomes; yellow arrows: p-p chromosome fusions without telomere at the site of fusions; green arrows: telomere signal-free chromosome ends. **(b)** Quantification of chromosome aberrations in *Rnf8*$^{+/+}$ and *Rnf8*$^{-/-}$ metaphases. A minimum of 30 metaphases were examined. Mean values were derived from at least three experiments. Error bars: s.d. **(c)** SV40LT immortalized *Rnf8*$^{+/+}$ and *Rnf8*$^{-/-}$ MEFs were treated with control vector or mTPP1$^{\Delta RD}$ for 120 h, metaphases were prepared and telomere aberrations visualized by Tam-OO-(CCCTAA)$_4$ telomere peptide nucleic acid (red) and DAPI (blue). Arrows: fused chromosomes. **(d)** Quantification of telomere fusion frequencies in *Rnf8*$^{+/+}$ and *Rnf8*$^{-/-}$ MEFs after expressing mTPP1$^{\Delta RD}$. A minimum of 1200 chromosomes were analyzed and mean values derived from at least three experiments are presented. Error bars: s.d. *P = 0.003, two-tailed Student's t-test. (**e**) SV40LT immortalized *Rnf8*$^{+/+}$ and *Rnf8*$^{-/-}$ MEFs were treated with control vector or shTrf2 for 120 h, metaphases prepared and telomere aberrations visualized by Tam-OO-(CCCTAA)$_4$ telomere peptide nucleic acid (red) and DAPI (blue). Arrows: fused chromosomes in *Rnf8*$^{-/-}$ MEFs treated with mTPP1$^{\Delta RD}$. The numerous fused chromosomes seen in *Rnf8*$^{+/+}$ MEFs treated with shTrf2 are not labeled. **(f)** Quantification of telomere fusion frequencies in *Rnf8*$^{+/+}$ and *Rnf8*$^{-/-}$ MEFs after *Trf2* depletion. A minimum of 1200 chromosomes were analyzed and mean values derived from at least three experiments presented. Error bars: s.d. *P = 0.01, **P = 0.003, two-tailed Student's t-test.

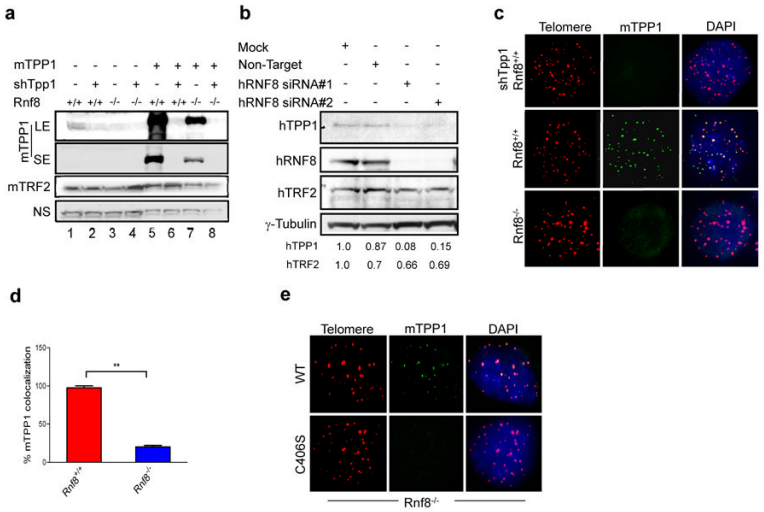

Figure 3. RNF8 is required for the accumulation of the TPP1-POT1a/b complex at telomeres

(a) *Rnf8*$^{+/+}$ and *Rnf8*$^{-/-}$ cell lysates were subjected to SDS-PAGE and Western blotting with the indicated antibodies. The specificity of the mouse TPP1 antibody is demonstrated by shRNA against mTPP1, which efficiently depleted both endogenous and exogenous mTPP1. γ-tubulin was used a loading control. (LE: long exposure, SE: short exposure). Quantification of TPP1 expression levels: lane 1–1.0, lane 2–0.41, lane 3–0.34, lane 4–0.20. Quantification of mTRF2 levels: lane 1–1.0, lane 2–1.0, lane 3–0.86, lane 4–1.2. **b)** HeLa cells transfected with two independent siRNAs against *RNF8* were harvested after 48 hours, subjected to SDS-PAGE and imunoblotted with anti-hRNF8, anti-hTPP1 and anti-hTRF2 antibodies. γ-tubulin was used as a loading control. Quantification of protein levels are as indicated. **(c)** *Rnf8*$^{+/+}$ and *Rnf8*$^{-/-}$ cells grown on coverslips were stained with anti-mTPP1 antibody (green), Tam-OO-$(CCCTAA)_4$ telomere peptide nucleic acid (red) and DAPI (blue). The specificity of the mouse TPP1 antibody for immunofluorscence is demonstrated in the upper panels by shRNA against mTPP1 **(d)**. Quantification of mTPP1 co-localized with Tam-OO-$(CCCTAA)_4$ telomere peptide nucleic acid. A minimum of 100 cells were examined mean values were derived from three experiments. Error bars: s.d. $^{**}P = 0.001$, two-tailed Student's *t*-test. **(e)** *Rnf8*$^{-/-}$ MEFs reconstituted with wild-type mRNF8 and the mRNF8^{C406S} RING mutant were stained with anti-mTPP1 antibody (green), Tam-OO-$(CCCTAA)_4$ telomere peptide nucleic acid (red) and DAPI (blue).

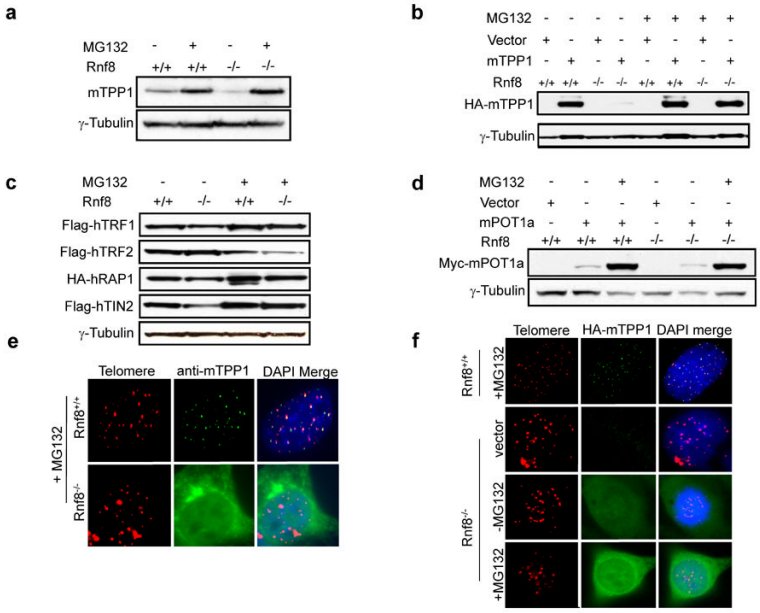

Figure 4. RNF8 is required for preventing TPP1 from proteasome-mediated degradation

(a) *Rnf8*$^{+/+}$ and *Rnf8*$^{-/-}$ MEFs were incubated in the presence or absence of 12.5μ-M of MG132 and lysates subjected to immunoblotting with anti-mTPP1 antibody. **(b)** Lysates isolated from *Rnf8*$^{+/+}$ and *Rnf8*$^{-/-}$ MEFs stably expressing HA-mTPP1 in the presence or absence of 12.5μ-M MG132 were subjected to immunoblotting with anti-HA antibody. γ-Tubulin used as a loading control. **(c)** *Rnf8*$^{+/+}$ and *Rnf8*$^{-/-}$ MEFs transfected individually with the indicated cDNA constructs in the presence or absence of 12.5μ-M of MG132 were subjected to immunoblotting with anti-FLAG and anti-HA and **(d)** anti-Myc antibodies. γ-Tubulin served as the loading control. **(e)** Cells grown on coverslips in the presence of 12.5 μm MG132 were fixed and stained with anti-mTPP1 (green), Tam-OO-$(CCCTAA)_4$ telomere peptide nucleic acid (red) and DAPI (blue). **(f)** *Rnf8*$^{+/+}$ and *Rnf8*$^{-/-}$ MEFs transfected with HA-mTPP1 and incubated in the presence or absence of 12.5μ-M of MG132 were subjected to immunofluorescence microscopy with anti-HA antibody (green), telomere-PNA FISH (red) and DAPI (blue).

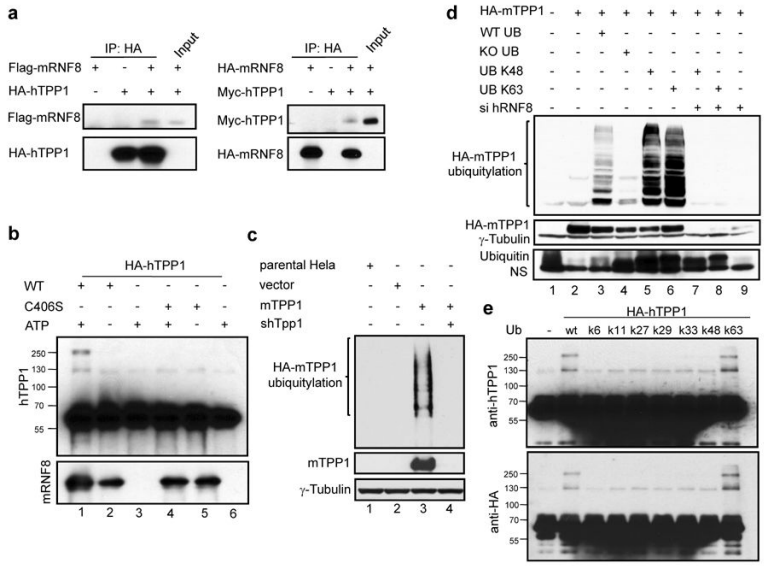

Figure 5. RNF8 physically interacts with and ubiquitylates TPP1

(a) 293T cells transfected with the indicated plasmids were immunoprecipitated with anti-HA antibody, subjected to SDS PAGE and western blotting with the indicated antibody. Input represent 5% of the total cell lysate used for the immunoprecipitations. **(b)** The ubiquitylation assay was performed with purified mRNF8^{WT} or the mRNF8^{C406S} RING mutant proteins, together with purified HA-hTPP1 protein and ubiquitin-activating enzyme (E1), MMS2 and Ubc13, RNF8, ubiquitin, ubiquitin aldehyde and ATP. Reaction mix subjected to immunoblotting to detect ubiquitylated hTPP1 with the anti-hTPP1 antibody. Anti-hRNF8 antibody used to show equal amount of hRNF8 used in the reactions. The HA-hTPP1-Ub species migrates at 250kD. **(c)** Stably infected mTPP1 in HeLa-UB cell line stably expressing treated with 2μg/ml biotin were harvested and incubated with strepavidin-agarose slurry. Washed beads eluted subjected to SDS-PAGE and Western blotting with the indicated antibodies. Stably infected mTPP1 cells co-infected with shTpp1 was used as a control to show the specificity of mTPP1 ubiquitylation. γ-tubulin was used as the loading control. Bracket indicates smear signals indicative of polyubiquitylation. **(d)** Lysates obtained from HeLa cells transfected with the indicated constructs or siRNF8 were incubated with nickel-NTA-agarose beads. Washed beads eluted subjected to SDS-PAGE and Western blotting with the indicated antibodies. Anti-HA and anti-ubiquitin antibodies were used to detect the expression of HA-mTPP1 and ubiquitin. γ-Tubulin was used as a loading control. **(e**) *In vitro* ubiquitylation assay performed as in **(b)** with either wild-type His-tagged ubiquitin or His-tagged ubiquitin mutants in which all lysines were mutated to arginines except for the one indicated. Reaction mix was subjected to immunoblotting with TPP1 (top panel) or anti-HA antibody (lower panel). The HA-hTPP1-Ub species migrates at 250kD.

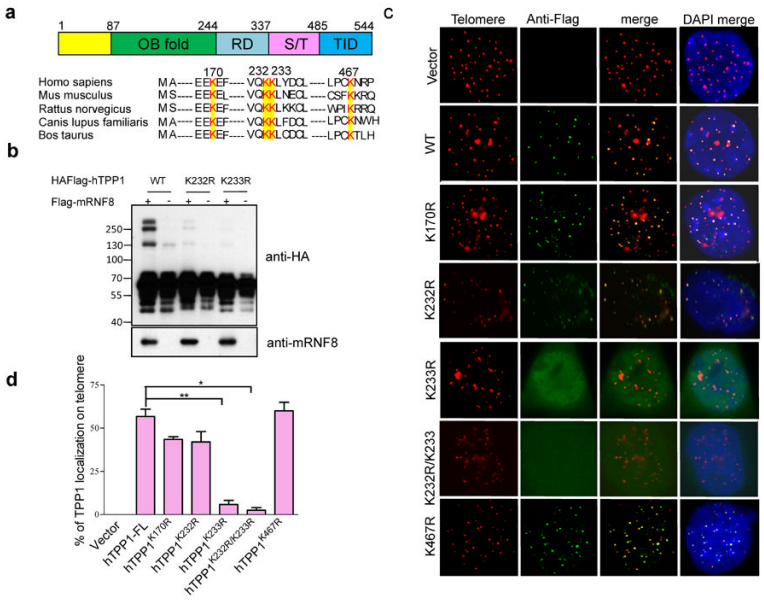

Figure 6. Lysine 233 is required for TPP1 ubiquitylation, telomere localization and genome stability

(a) Schematic representation of the conserved lysine residues in hTPP1 across the species (lysine residue mutated are highlighted in yellow). **(b)** Lysine K233 is required for hTPP1 ubiquitylation. *In vitro* ubiquitylation assay in the presence and absence of purified wild-type mRNF8 with either wild type HA-hTPP1 or indicated lysine to arginine HA-hTPP1 mutants. Reaction mix was subjected to immunoblotting with anti-HA antibody. The HA-hTPP1-Ub species migrates at 250kD. Bottom panel is a short exposure to show equal amounts of TPP1 proteins used in the assay. **(c)** Telomere-PNA FISH showing the localization of exogenous hTPP1 lysine mutants in *Rnf8*$^{+/+}$ MEFs. Cells stably infected with FLAG-tagged wild-type or indicated hTPP1 mutants were stained with anti- FLAG antibody (green), Tam OO- $(CCCTAA)_4$ telomere peptide nucleic acid (red) and DAPI (blue). **(d)** Quantification of localization of wild-type and mutant hTPP1 on telomeres. A minimum of 200 cells were examined mean values were derived from three experiments. Error bars: s.d. *$P = 0.001$, **$P = 0.0006$, two-tailed Student's t-test.